An Anion-Selective Analogue of the Channel-Forming Peptide Alamethicin[†]

Andrei V. Starostin,[‡] Radu Butan,[‡] Vitali Borisenko,[‡] D. Andrew James,[‡] Holger Wenschuh,[§] Mark S. P. Sansom,[||] and G. Andrew Woolley*,[‡]

Department of Chemistry, University of Toronto, 80 St. George Street, Toronto M5S 3H6, Canada, Jerini BioTools, 12489 Berlin, Germany, and Laboratory of Molecular Biophysics, Department of Biochemistry, University of Oxford, South Parks Road, Oxford OX1 3QU, U.K.

Received November 5, 1998; Revised Manuscript Received February 25, 1999

ABSTRACT: The peptide alamethicin self-assembles to form helix bundle ion channels in membranes. Previous macroscopic measurements have shown that these channels are mildly cation-selective. Models indicate that a source of cation selectivity is a zone of partial negative charge toward the C-terminal end of the peptide. We synthesized an alamethicin derivative with a lysine in this zone (replacing the glutamine at position 18 in the sequence). Microscopic (single-channel) measurements demonstrate that dimeric alamethicin-lysine18 (alm-K18) forms mildly anion-selective channels under conditions where channels formed by the parent peptide are cation-selective. Long-range electrostatic interactions can explain the inversion of ion selectivity and the conductance properties of alamethicin channels.

Ion selectivity is a critical feature of ion channels and is essential to the normal functioning of biological membranes. An elementary level of selectivity is charge selectivity, the ability of a channel to discriminate between ions with opposite charges (e.g., K^+ vs Cl^-). Fundamentally, selectivity must be a consequence of the energetics and kinetics of the interactions between the ions, the channel, and water. This can be a complicated physicochemical system, however, so it has been difficult to predict what kind of selectivity will result even when a detailed structural model of a channel is available. For example, in the case of gramicidin, there is an ongoing debate about the origin of charge selectivity, i.e., whether this arises from differential protein−ion interactions or ion−water interactions (*1*−*3*).

We have focused on understanding the permeation properties of a relatively simple system, the alamethicin channel (*4*, *5*). Alamethicin monomers or dimers (Figure 1) adopt helical secondary structures. These self-assemble in membranes into ion-conducting helix bundles (*6*). Alamethicin channels have served as models for protein helix bundle channels such as those belonging to the acetylcholine receptor family.

The relative permeation rates of various ions through alamethicin channels parallel their relative diffusion rates in bulk solution (*7*). In addition, channel conductance does not appear to saturate as the ion concentration is increased (*8*). These observations suggest that continuum diffusion effects, rather than ion binding events at discrete sites, dominate the movement of ions through these channels. Furthermore, these observations suggest that the charge selectivity of the channels will be dominated by long-range electrostatic interactions (*9*, *10*). Such interactions can be described by a Poisson−Boltzmann model, given an appropriate structure (*11*−*16*).

Detailed structural models of the alamethicin channel have been developed previously (*17*, *18*). These models were used to calculate electrostatic energy profiles for a cation (or anion) along a trajectory through the pore by numerically solving the linearized Poisson−Boltzmann equation for a series of salt concentrations (*8*). Rigorous calculations of detailed electrostatic potential profiles in the presence of a salt gradient, however, present a number of complications (*19*, *20*). Nevertheless, electrostatic calculations can still identify zones of channel charge that may act as sources of cation versus anion selectivity. Alamethicin channels exhibit a broad zone of favorable electrostatic interactions between a cation and the pore in the region from the glycine at position 11 to the C-terminus (*8*). The glutamine side chains at position 18 as well as the kinked peptide backbone appear to contribute to these interactions. A favorable, although less pronounced, interaction with anions also occurs at the N-terminus due to helix dipoles.

Macroscopic measurements have been reported that indicate alamethicin channels are cation-selective. Eisenberg et al. and Menestrina et al. (*7*, *21*, *22*) measured reversal potentials for alamethicin Rf30 (Glu-18) channels in KCl salt gradients. The orientation of the channels with respect to the salt gradient is likely the same as in the case described here (see below). A macroscopic selectivity ($P_{K^+}/P_{Cl^-} = 2.7$) was observed. Hall et al. (*23*) performed qualitative macroscopic selectivity measurements by applying voltage steps and recording current decays in KCl gradients. Several derivatives, including a methyl ester of alm-Rf30[1] [which should behave in a manner similar to that of alm-Rf50 (Gln-18)], were reported to be cation-selective, although permeability ratios were not calculated. Surface potentials have

[†] This work has been supported by the Canadian Cystic Fibrosis Foundation.

* Corresponding author. E-mail: awoolley@chem.utoronto.ca. Telephone and fax: (416) 978-0675.

[‡] University of Toronto.

[§] Jerini BioTools.

[||] University of Oxford.

10.1021/bi9826355 CCC: $18.00 © 1999 American Chemical Society
Published on Web 04/22/1999

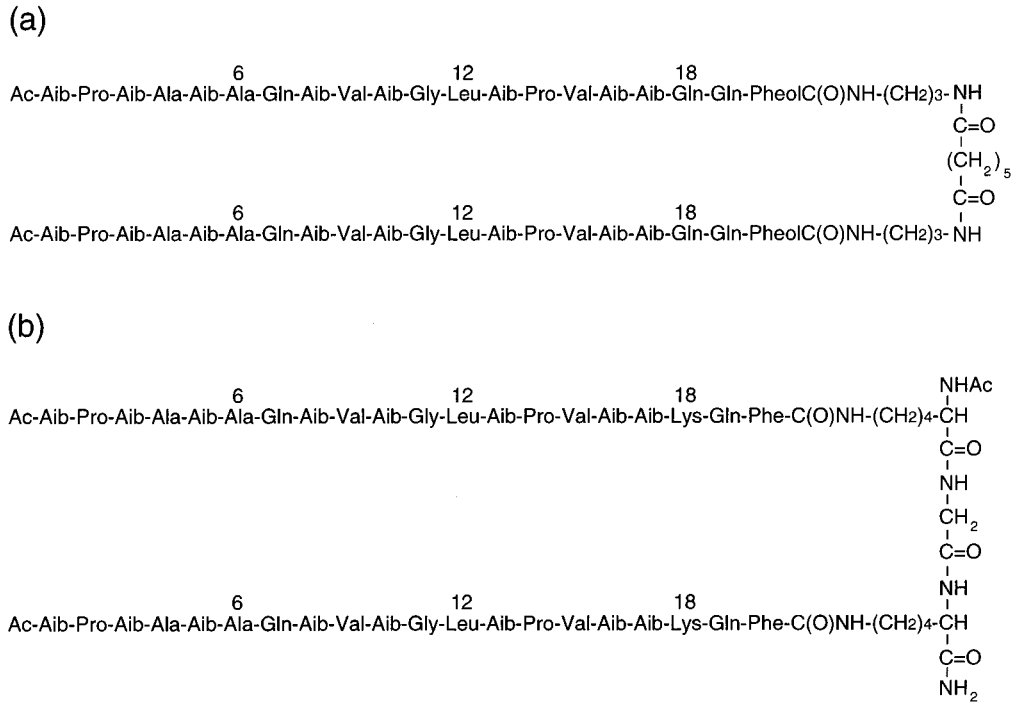

FIGURE 1: Primary structure of (a) alamethicin bis(*N*-3-aminopropyl)-1,7-heptanediamide (alm-BAPHDA, or alm-Q18) and (b) alamethicin-lysine 18 (alm-K18). Alm-Q18 has glutamine at position 18 (Q-18) and is used here as the standard for comparison. Monomeric forms of the peptides terminate after residue 20. Alamethicin Rf30 (used in previous macroscopic measurements) has glutamate at position 18.

also been reported to affect alamethicin charge selectivity (*24*).

To test the role of long-range electrostatics in determining alamethicin charge selectivity, we decided to attempt to engineer a change in selectivity from cation-selective to anion-selective. To assess the charge selectivity experimentally, we focused exclusively on microscopic (single-channel) conductance measurements. Whereas the macroscopic charge selectivity measurements described above reflect the selectivity properties of an ensemble of structures, single-channel measurements permit selectivity to be related to specific conducting structures. We synthesized a dimeric alamethicin derivative (alm-K18) with lysine replacing glutamine at position 18 in the sequence. This derivative was found to form mildly anion-selective channels under conditions where channels formed by the parent peptide are cation-selective.

EXPERIMENTAL PROCEDURES

Peptide Synthesis. Alm-K18 dimers were obtained via stepwise solid-phase assembly of two parallel (monomeric) alamethicin-K18 chains on an Ac-Lys-Gly-Lys-NH_2 template. Initially, the template was synthesized using a TG-S RAM resin (Rapp Polymere, Tübingen, Germany; loading of 0.24 mmol/g) on a model 433A peptide synthesizer (Applied Biosystems, Weiterstadt, Germany). Double couplings (30 min) were applied using 8 equiv of Fmoc amino acids, 8 equiv of HATU, and 16 equiv of DIEA at a coupling concentration of 0.3 M (amino acid) in DMF. The DDE group was used for orthogonal protection for the Lys side chain function. Before deprotection of the DDE group with 2% hydrazine/DMF (2 × 10 min), the N-terminus was acetylated using an acetic anhydride/DIEA/DMF mixture (1:2:7) for 30 min. The alamethicin-K18 chains were then assembled using 8 equiv of isolated Fmoc amino acid fluorides (*25*) and 8 equiv of DIEA at a concentration of 0.3 M (amino acid) in DMF. Double couplings (2 × 45 min) were performed.

At the end of the synthesis, the N-terminal amino function was acetylated using the protocol described above. Peptide resin cleavage was performed with a solution of 2% triisopropylsilane and 5% water in 50% TFA/DCM for 50 min. The product was precipitated in diethyl ether and purified by preparative HPLC (Polyencap A300 column, 4.6 mm × 125 mm, linear gradient, eluant A being 0.1% TFA in water, eluant B being 0.1% TFA in 80% acetonitrile/20% water). Prior to being used in single-channel measurements, the peptide was rechromatographed under the same conditions using an analytical-scale column of the same type. The peptide was analyzed by HPLC and MALDI-MS. The purity as determined by HPLC was >97%. MALDI-MS data: Ac-Lys-(alamethicin-K18)-Gly-Lys-(alamethicin-K18)-NH_2 calcd 4291.3 $[M + H]^+$, found 4313.1 $[M + Na]^+$.

Single-Channel Measurements. Typically, 3−5 μL of peptide solution (~0.05 mg/mL in MeOH) was added to both sides of membranes formed from diphytanoylphosphatidylcholine/decane (50 mg/mL). Polystyrene bilayer chambers with 150 μm apertures (Warner Instrument Co.) were employed. Currents were measured, and the voltage was set using an Axopatch 1D patch-clamp amplifier (Axon Instruments) controlled by Synapse (Synergistic Research Systems). A CV-4B-0.1/100 switchable headstage was em-

[1] Abbreviations: alm, alamethicin; BAPHDA, bis(*N*-3-aminopropyl)-1,7-heptanediamide; BES, *N*,*N*-bis(2-hydroxyethyl)-2-aminoethanesulfonic acid; DCM, dichloromethane; DIEA, diisopropylethylamine; DMF, dimethylformamide; MALDI-TOF, matrix-assisted laser desorption time-of-flight; Fmoc, 9-fluorenylmethyloxycarbonyl; HATU, *O*-(7-azabenzotriaol-1-yl)-*N*,*N*,*N*′,*N*′-tetramethyluronium hexafluorophosphate; HPLC, high-performance liquid chromatography; *I*−*V*, current−voltage; K^+Glu^-, potassium gluconate; MeOH, methanol; Nmg^+Cl^-, *N*-methyl-D-glucosamine chloride; TFA, trifluoroacetic acid.

ployed, with the headstage gain set at 0.1. Data were filtered at either 2 or 1 kHz, sampled at 5 times the filter frequency, stored directly to disk, and analyzed using Synapse and Igor (Wavemetrics, Inc.). All measurements were taken at 22 ± 2 °C. Salt solutions were connected via agarose/KCl salt bridges to KCl (1.3 M) reservoirs containing silver/silver chloride electrodes. All KCl solutions contained 5 mM BES (pH 6.8). Nmg^+Cl^- and K^+Glu^- solutions were buffered with 5 mM BES to pH 7 by addition of KOH or HCl. Conductances of bulk solutions were measured using a Wheatstone bridge as described by Shoemaker et al. (*26*).

Single-channel current−voltage (*I*−*V*) curves were obtained using the following voltage-clamp protocol: a step from 0 to 200 mV, holding at 200 mV for 50−500 ms, then a ramp to −200 mV over the course of 20−80 ms, followed by a return to 0 mV for several seconds. Capacitative currents obtained when no channels were opened were subtracted from currents obtained with a single channel open during the ramp. With ramp times of ≥20 ms and the amplifier settings described above, the capacitative transient did not lead to amplifier saturation.

This protocol measures the *I*−*V* relationship for channels oriented with their N-terminus at the high-salt side of the membrane since the high-salt (1.3 M KCl) side is always at electrical ground and the N-terminus inserts through the membrane from the side made positive by the applied field (*8*, *27*). Figures 4 and 5 show several individual ramps (*I*−*V* curves) superimposed. The ramps have not been averaged or smoothed (except by the amplifier filter) so that the variability and noise shown in the plots directly represent the experimental variability. The number of ramps (*n*) superimposed in each case is indicated in the figure legends. Smooth polynomial curves are drawn through the points as a visual aid only.

Permeability ratios were calculated from reversal potentials as described by Lear et al. (*28*). Activity coefficients for KCl solutions were taken from Robinson and Stokes (*29*). Plots of chord conductances versus voltage were obtained by dividing the measured current by the measured voltage using the data analysis program Igor (Wavemetrics, Inc.).

Molecular Modeling and Electrostatic Calculations. Alamethicin models were generated by restrained molecular dynamics simulations as described previously (*17*, *18*). These were subsequently employed in calculations of pK_as of ionizable (lysine) residues using the procedure described in detail by Adcock et al. (*30*). Electrostatic potential profiles and single-channel *I*−*V* relationships were then estimated as described by Woolley et al. (*8*).

RESULTS AND DISCUSSION

Peptide Synthesis. We synthesized an analogue of alamethicin with lysine at position 18 [alm-K18 (Figure 1)]. Position 18 is a pore-lining site that should not interfere directly with helix−helix packing. A dimeric peptide, rather than a monomer, was constructed because previous studies had demonstrated that dimerization leads to extended single-channel lifetimes (*18*). Extended lifetimes are required to make measuring single-channel *I*−*V* relationships practical. The linker for the dimeric peptide (Figure 1) was chosen to resemble as closely as possible previously employed linkers. Small differences in the linkers are not expected to affect the channel conductance properties significantly (*31*).

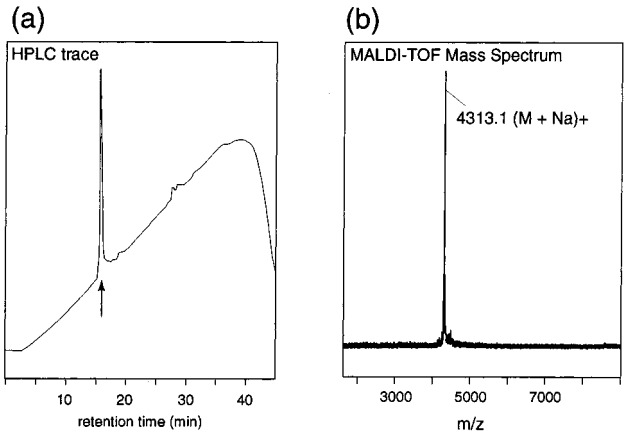

FIGURE 2: (a) HPLC chromatogram of the alm-K18 dimer. A linear gradient from 50 to 80% solvent B over the course of 35 min was used (solvent A being 0.1% TFA in water, and solvent B being 0.1% TFA in 80% acetonitrile/20% water), at a flow rate of 0.8 mL/min, with a t_R of 17 min. The peak denoted by the arrow was collected and used for single-channel measurements. (b) MALDI-TOF mass spectrum of the HPLC-purified alm-K18 dimer.

Synthesis of the complete dimer on a solid support was found to be a superior approach to dimerization of separately synthesized alm-K18 monomers (data not shown). Incomplete dimerization with the latter procedure led to peptide mixtures that proved to be difficult to separate using HPLC. In Figure 2 are shown an HPLC chromatogram (a) and a MALDI-TOF mass spectrum (b) of the alm-K18 peptide synthesized entirely on the solid support and then purified in preparation for single-channel measurements.

Channel Properties in Symmetrical KCl Solutions. In Figure 3a is shown a constant-voltage current recording of channels formed by the alm-K18 dimer (1 M KCl, 200 mV). The pattern of channel formation is typical for a dimeric alamethicin derivative; even-numbered conducting bundles are selectively stabilized (panel b) (*31*). The lifetimes of individual states appear to be somewhat reduced compared to those of the corresponding states of the (uncharged) alm-Q18 (Gln-18, alm-BAPHDA) channel (*18*), although a full analysis is beyond the scope of this report.

The current−voltage (*I*−*V*) relationship of the putative hexamer level (*18*) of the alm-K18 dimer in 1 M KCl is compared to that of the alm-Q18 dimer in Figure 4a. At positive voltages (the N-terminus is at ground), the observed current for alm-K18 is smaller than for alm-Q18. For negative voltages, however, the current is larger. A plot of chord conductance versus voltage (Figure 4b) shows clearly that the alm-K18 peptide does not rectify as strongly as the native alm-Q18 channel.

The origin of rectification in the alm-Q18 channel appears to be the asymmetric distribution of charge along the channel axis (*8*). There is an electrostatic barrier for cations at the N-terminus and a potential well toward the C-terminus. The opposite is true for anions. In the alm-K18 channel, the electrostatic field generated by the lysine residues should negate, to some extent, the potential well for cations (see below). The electrostatic potential profile will then be more uniform along the length of the channel. A more uniform electrostatic profile is expected to produce more linear *I*−*V* curves, i.e., less rectification (*8*).

Charge Selectivity Measured in a KCl Gradient. Charge selectivity was assessed by measuring *I*−*V* relationships in

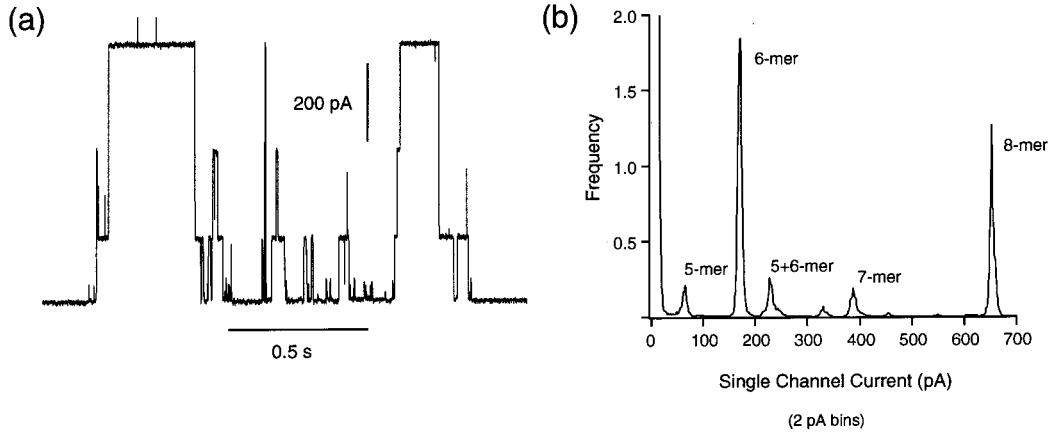

FIGURE 3: Properties of alm-K18 channels in symmetrical 1 M KCl solutions (5 mM BES at pH 6.8): (a) single-channel current events at a constant voltage (200 mV) and (b) the frequency of occurrence of different current levels (200 mV).

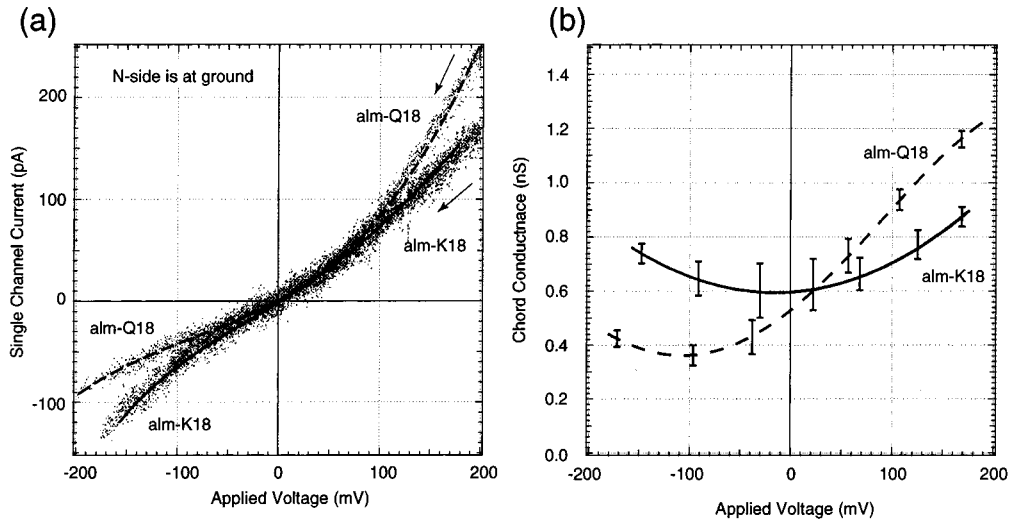

FIGURE 4: Comparison of the conductance properties of alm-K18 channels and alm-Q18 channels in symmetrical 1 M KCl solutions (5 mM BES at pH 6.8). (a) Single-channel $I-V$ curves of alm-K18 (solid line) and alm-Q18 (dashed line). The direction of the voltage ramps is indicated by the arrows. The number of $I-V$ ramps superimposed for alm-Q18 was seven and for alm K-18 was five. Transitions to closed states have been eliminated for clarity. (b) Chord conductances calculated from the data shown in panel a. The alm-K18 dimer rectifies much less strongly than alm-Q18.

KCl salt gradients. In Figure 5 are shown $I-V$ relationships for alm-Q18 and alm-K18 in the presence of a 0.1 to 1.3 M KCl gradient (panel a) and a 0.01 to 1.3 M KCl gradient (panel b). The reversal potential observed for alm-Q18 in the latter case (panel b) is 35 mV, indicating that alm-Q18 is cation-selective with a P_{K^+}/P_{Cl^-} of 4.3. The observed reversal potential for alm-K18 (−32 mV) gives a permeability ratio P_{Cl^-}/P_{K^+} of 3.7, similar in magnitude, but opposite in sign, to that of alm-Q18. That is, alm-K18 is anion-selective. With the smaller ion gradient (0.1 to 1.3 M KCl, panel a), a similar result is obtained (for alm-Q18, $P_{K^+}/P_{Cl^-} = 2.1$; for alm-K18, $P_{Cl^-}/P_{K^+} = 1.8$), but the observed permeability ratios are somewhat lower. The decreased selectivity with the smaller KCl gradient is presumably a result of an increased level of screening of charge on the peptides by the higher-ionic strength solution (0.1 vs 0.01 M KCl at the C-terminal side of the membrane).

This particular alamethicin-conducting state has tentatively been assigned to a bundle of eight helices (four dimers) (*18*). The putative hexamer level exhibits a similar selectivity (data not shown). The observed selectivity of alm-Q18 was sensitive to the orientation of the salt gradient relative to the (asymmetric) channel, as has been found for the Leu-Ser series of helix bundle peptides studied by Kienker et al. (*2*, *32*). Anion selectivity was observed with alm-K18, however, with either orientation of the salt gradient.

The single-channel charge selectivity of alm-Q18 measured under the conditions described in the legend of Figure 5 is similar to the macroscopic selectivity ($P_{K^+}/P_{Cl^-} = 2.7$) reported by Eisenberg et al. (*7*) for the naturally occurring glutamate-containing alamethicin derivative Rf30 (alm-E18). Even if it were incompletely ionized,[2] a glutamic acid residue at position 18 (alm-E18) might be expected to increase the negative charge density in the C-terminal zone and so contribute to increased cation selectivity. Conversely, helix bundles larger than the octamer occurring in a macroscopic ensemble might be expected to exhibit lower levels of charge selectivity. The macroscopic permeability ratio P_{K^+}/P_{Cl^-} of 2.7 presumably reflects a weighted average of the single-channel charge selectivities of the members of the conducting ensemble.

[2] As is suggested by calculations of glutamic acid pK_as in alm-Rf30 bundles (*33*).

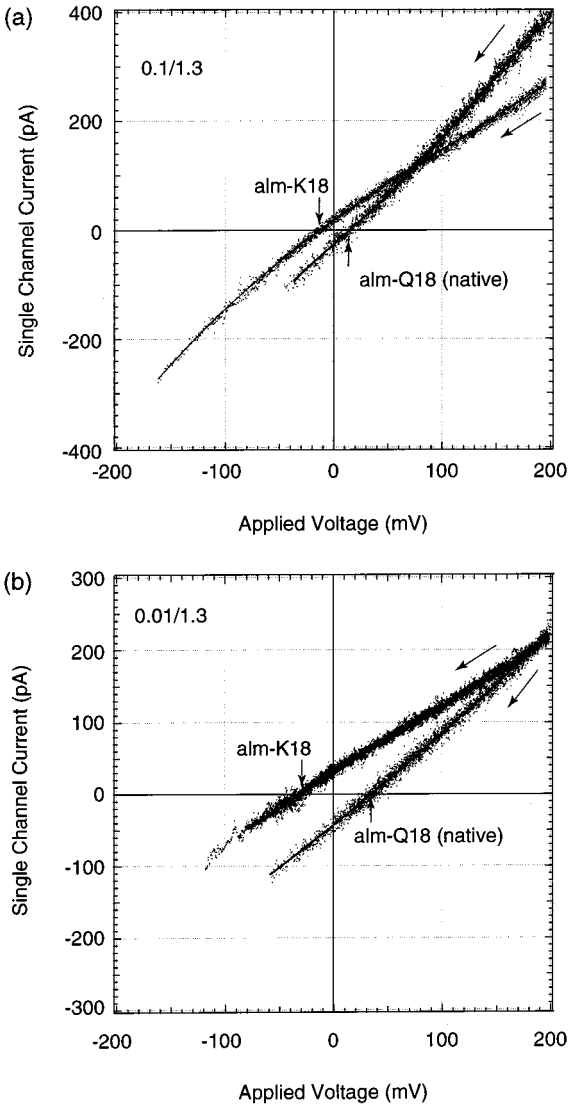

FIGURE 5: Single-channel current−voltage ($I-V$) curves for the octamer level of alm-Q18 (linked with the BAPHDA group) and dimeric alm-K18 (Figure 1) channels. Channels opened at 200 mV, whereupon the voltage was ramped to −200 mV (as indicated by the long arrows) over 20−80 ms and the current recorded. Channels generally closed before the voltage reached −200 mV. Capacitive currents recorded when no channels were opened were subtracted as described in Experimental Procedures. The KCl concentration was 1.3 M on the grounded side and either 0.1 (panel a) or 0.01 M (panel b) on the other side with 5 mM BES at pH 6.8 on each side. Channels are oriented so that the N-terminal side is at ground. Reversal potentials are indicated. The number of $I-V$ ramps superimposed (a) for alm-Q18 was eight and for alm K-18 was ten and (b) for alm-Q18 was eight and for alm-K18 was eleven. Transitions to closed states have been eliminated for clarity.

Charge Selectivity Measured Using Bulky Counterions. As another measure of charge selectivity, single-channel measurements were taken using solutions of potassium gluconate (K^+Glu^-) and *N*-methylglucosammonium chloride (Nmg^+Cl^-). In both solutions, the majority of the current is expected to be carried by the smaller ion. Bulk conductivity measurements of 1 M solutions of K^+Glu^- and Nmg^+Cl^- gave similar values for equivalent conductance (45.6 and 44.1 Ω^{-1} mol^{-1} cm^2, respectively). Thus, K^+ ions are about as mobile in a solution of K^+Glu^- as Cl^- ions are in a solution of Nmg^+Cl^-. The relative magnitudes of single-channel currents measured in K^+Glu^- and Nmg^+Cl^- solutions should therefore depend primarily on the relative permeability of the channel for K^+ and Cl^- ions.

Table 1: Single-Channel Currents in Nmg^+Cl^- and K^+Glu^- Solutions

peptide	salt solution[a]	record time (s)[b]	6-mer (pA)[c]	7-mer (pA)	8-mer (pA)
alm-Q18	K^+Glu^-	293	61 ± 7	142 ± 7	235 ± 10
alm-Q18	Nmg^+Cl^-	183	49 ± 7	124 ± 8	210 ± 12
alm-K18	K^+Glu^-	131	30 ± 12	75 ± 20	155 ± 15
alm-K18	Nmg^+Cl^-	93	55 ± 10	130 ± 7	220 ± 10

[a] Salt solutions (1 M) were employed with an applied potential of 200 mV. [b] Total recording time (channels were open at some current level more than 50% of the time). [c] As discussed in the text, the molecularity of particular current levels is tentatively assigned.

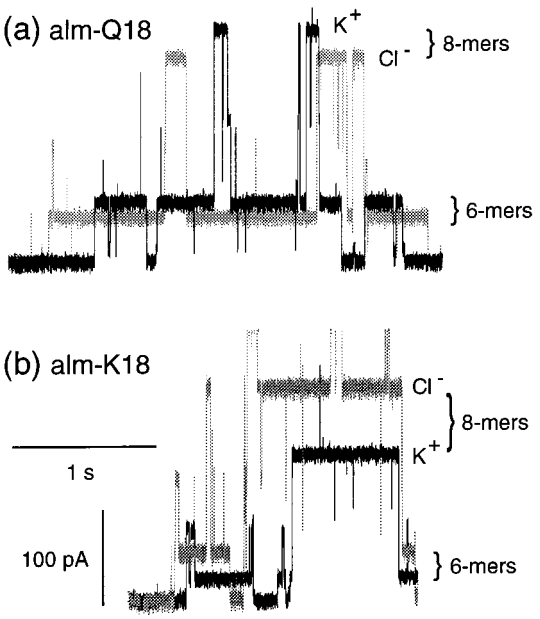

FIGURE 6: Single-channel recordings of alm-Q18 (a) and alm-K18 (b) in 1 M solutions of K^+Glu^- (black) and Nmg^+Cl^- (gray). Each solution also contained 5 mM BES buffer (pH 7). Octameric and hexameric levels are indicated.

Continuous records of single-channel events were obtained for alm-Q18 and alm-K18 in 1 M solutions of K^+Glu^- and Nmg^+Cl^- at an applied potential of 200 mV. Observed current levels are collected in Table 1. Sections of the records are plotted together in Figure 6a (alm-Q18) and Figure 6b (alm-K18) to facilitate a visual comparison of the selectivities. With alm-Q18 channels (Figure 6a), the single-channel current is higher in K^+Glu^- than in Nmg^+Cl^- but only marginally ($I_{K^+}/I_{Cl^-} = 1.2$ for the hexamer level and $I_{K^+}/I_{Cl^-} = 1.1$ for the octamer level). In alm-K18 channels (Figure 6b), however, the Cl^--mediated current is significantly higher than the K^+-mediated one ($I_{Cl^-}/I_{K^+} = 1.8$ for the hexamer, and $I_{Cl^-}/I_{K^+} = 1.4$ for the octamer).

The sizes of the Cl^--mediated current in the alm-K18 channels and the Cl^--mediated current in the alm-Q18 channels are similar (Figure 6 and Table 1). The K^+-mediated current in the alm-K18 channels, however, is significantly reduced. Thus, it appears that the Cl^- selectivity of alm-K18 occurs primarily as a result of a decreased K^+ permeability of alm-K18 relative to that of alm-Q18. The lower current observed for K^+ in alm-K18 channels is unlikely to be due to a misidentification of (for example) the 8-mer level

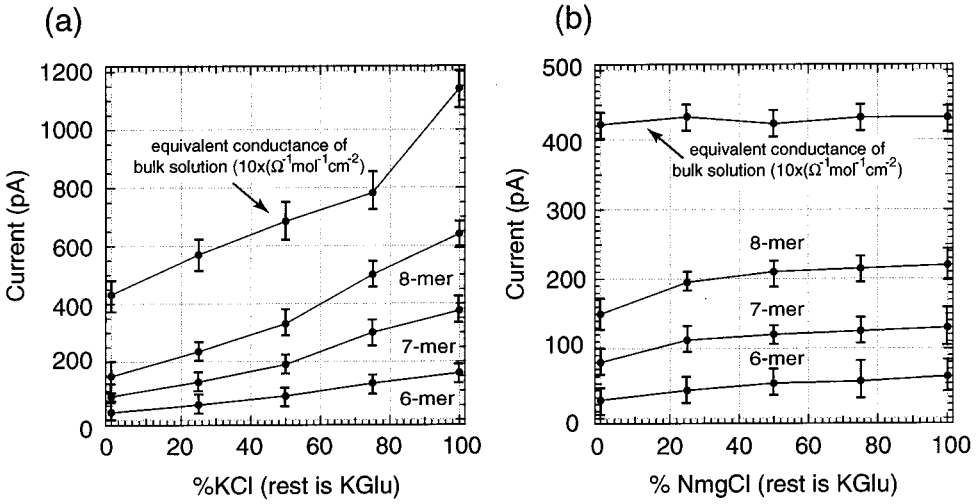

FIGURE 7: Single-channel currents of alm-K18 in mixed salt solutions. A 1 M solution of K^+Glu^- was mixed with 1 M solutions of KCl (a) or Nmg^+Cl^- (b) in the proportions indicated. Single-channel currents were measured as described in the text. Bulk equivalent conductances (in the indicated units) are plotted on the same scale for reference.

as a 7-mer because the levels above and below the indicated 8-mer have shorter lifetimes (as expected for an even-numbered level).

To confirm that the current levels were correctly identified, we performed a series of single-channel current measurements where K^+Glu^- and KCl (or Nmg^+Cl^-) solutions were combined in different proportions. Figure 7 (upper lines in panels a and b) demonstrates that the bulk conductivities of these mixed salt solutions are approximately linearly dependent on the concentrations of each component. In K^+-Glu^-/KCl mixtures (panel a), we reasoned that if the single-channel current levels were correctly identified, they should approximately parallel the bulk conductivity as the proportion of one salt is systematically increased. This is observed to be the case (Figure 7a). If a level were misidentified, the currents for that level would show a dependence on the percentage of KCl that was distinctly different from the bulk. Figure 7b shows the results from an analogous experiment where the proportions of K^+Glu^- and Nmg^+Cl^- were varied. Since the bulk conductivities of 1 M solutions of K^+Glu^- and Nmg^+Cl^- are very similar, the single-channel currents should only reflect the relative permeability for K^+ versus Cl^-. Here too, there are no abrupt changes in the current as the percentage of K^+Glu^- varies, which, if they occurred, would indicate a level misidentification. Instead, a gradual increase in current is observed as the percentage of Nmg^+Cl^- is increased, consistent with a greater permeability of the alm-K18 channel for Cl^- than for K^+.

Origins of Selectivity. These results appear to confirm the prediction that, at least for these conducting levels of the alamethicin pore,[3] charge selectivity is dominated by long-range electrostatic interactions. Of course, one cannot be sure that a change in pore structure has not occurred as a result of the glutamine to lysine mutation. Indeed, a change in structure must have occurred, at least locally. It would be surprising, however, that a change in pore structure alone would have coincidentally resulted in a switch in charge selectivity in the direction predicted on electrostatic grounds.

If ion permeation in alamethicin is dominated by long-range electrostatics, then an understanding of ion selectivity based on a structural model of the pore may be possible. Because the alamethicin channel assembles from identical subunits, the electrostatic character of the pore is approximately cylindrically symmetric. It is primarily the position along the long axis of the pore that determines the electrostatic energy of a permeating ion. Where cylindrical symmetry does not exist (e.g., in porins), an electrostatic description of ion selectivity will be more complicated (*12*).

For a quantitative electrostatic description of the alm-K18 pore to be made, the ionization state(s) of the lysine residues must be known. Preliminary electrostatics calculations based on an octameric alm-K18 pore model suggest that ca. four of the eight lysine residues will be positively charged at neutral pH. Current−voltage curves calculated using this assumption are approximately linear (i.e., no rectification) and indicate an anion:cation selectivity ratio of about 2. Both of these predictions agree with the experimental observations. In contrast, if all eight lysine residues are assumed to be positively charged, the channel is predicted to rectify strongly and have a much higher anion:cation selectivity ratio. If none of the lysine residues are charged, the channel is predicted to be cation-selective. Thus, it would seem the most likely state of the channel is one in which half of the lysines are ionized.

The results presented here imply that rational design based on electrostatic modeling of alamethicin pores could be a fruitful approach for generating channels that displayed higher degrees of charge selectivity. Analogues could be designed and synthesized that incorporated more extreme changes of channel charge distribution. Highly anion-selective alamethicin analogues could prove to be useful as tools for manipulating cellular anion permeability (*35*).

ACKNOWLEDGMENT

We acknowledge Prof. Gilles Lajoie for helpful discussions and the referees for helpful comments.

REFERENCES

1. Roux, B. (1996) *Biophys. J. 71*, 3177−3185.

[3] Very low conducting states have been reported to exhibit more pronounced ion selectivity (*34*).

2. Kienker, P. K., and Lear, J. D. (1995) *Biophys. J. 68*, 1347−1358.
3. Dorman, V., Partenskii, M. B., and Jordan, P. C. (1996) *Biophys. J. 70*, 121−134.
4. Cafiso, D. S. (1994) *Annu. Rev. Biophys. Biomol. Struct. 23*, 141−165.
5. Sansom, M. S. P. (1993) *Eur. Biophys. J. 22*, 105−124.
6. Woolley, G. A., and Wallace, B. A. (1992) *J. Membr. Biol. 129*, 109−136.
7. Eisenberg, M., Hall, J. E., and Mead, C. A. (1973) *J. Membr. Biol. 14*, 143−176.
8. Woolley, G. A., Biggin, P. C., Schultz, A., Lien, L., Jaikaran, D. C. J., Breed, J., Crowhurst, K., and Sansom, M. S. P. (1997) *Biophys. J. 73*, 770−778.
9. Levitt, D. G. (1991) *Biophys. J. 59*, 271−277.
10. Levitt, D. G. (1991) *Biophys. J. 59*, 278−288.
11. Dieckmann, G. R., Lear, J. D., Zhong, Q., Klein, M., DeGrado, M. L., and Sharp, K. A. (1999) *Biophys. J. 76*, 618−630.
12. Karshikoff, A., Spassov, V., Cowan, S. W., Ladenstein, R., and Schirmer, T. (1994) *J. Mol. Biol. 240*, 372−384.
13. Sansom, M. S. P. (1998) *Curr. Opin. Struct. Biol. 8*, 237−244.
14. Weetman, P., Goldman, S., and Gray, C. G. (1997) *J. Phys. Chem. B 101*, 6073−6078.
15. Warshel, A., and Papazyan, A. (1998) *Curr. Opin. Struct. Biol. 8*, 211−217.
16. Honig, B., and Nicholls, A. (1995) *Science 268*, 1144−1149.
17. Breed, J., Biggin, P. C., Kerr, I. D., Smart, O. S., and Sansom, M. S. P. (1997) *Biochim. Biophys. Acta 1325*, 235−249.
18. You, S., Peng, S., Lien, L., Breed, J., Sansom, M. S. P., and Woolley, G. A. (1996) *Biochemistry 35*, 6225−6232.
19. Roux, B. (1997) *Biophys. J. 73*, 2980−2989.
20. Chen, D., and Eisenberg, R. (1993) *Biophys. J. 64*, 1405−1421.
21. Menestrina, G., Voges, K. P., Jung, G., and Boheim, G. (1986) *J. Membr. Biol. 93*, 111−132.
22. Eisenberg-Grunberg, M. (1973) Ph.D. Thesis, California Institute of Technology, Pasadena, CA.
23. Hall, J. E., Vodyanoy, I., Balasubramanian, T. M., and Marshall, G. R. (1984) *Biophys. J. 45*, 233−248.
24. Mueller, P., and Rudin, D. O. (1968) *Nature 217*, 713−719.
25. Wenschuh, H., Beyermann, M., Krause, E., Brudel, M., Winter, R., Schumann, M., Carpino, L. A., and Bienert, M. (1994) *J. Org. Chem. 59*, 3275−3280.
26. Shoemaker, D. P., Garland, C. W., and Nibler, J. W. (1989) *Experiments in Physical Chemistry*, 5th ed., McGraw-Hill, New York.
27. Rink, T., Bartel, H., Jung, G., Bannwarth, W., and Boheim, G. (1994) *Eur. Biophys. J. 23*, 155−165.
28. Lear, J. D., Schneider, J. P., Kienker, P. K., and DeGrado, W. F. (1997) *J. Am. Chem. Soc. 119*, 3212−3217.
29. Robinson, R. A., and Stokes, R. H. (1968) *Electrolyte Solutions*, 2nd ed., Butterworths, London.
30. Adcock, C., Smith, G. R., and Sansom, M. S. P. (1998) *Biophys. J. 75*, 1211−1222.
31. Jaikaran, D. C., Biggin, P. C., Wenschuh, H., Sansom, M. S. P., and Woolley, G. A. (1997) *Biochemistry 36*, 13873−13881.
32. Woolley, G. A., Starostin, A., Butan, R., James, D., Wenschuh, H., and Sansom, M. (1998) in *Novartis Foundation Symposium 225* (Cardew, G., and Wallace, B., Eds.) John Wiley & Sons, London (in press).
33. Tieleman, D. P., Breed, J., Berendsen, H. J. C., and Sansom, M. S. P. (1998) *Faraday Discuss. 111* (in press).
34. Hanke, W., and Boheim, G. (1980) *Biochim. Biophys. Acta 596*, 456−462.
35. Woolley, G. A., Pfeiffer, D. R., and Deber, C. M. (1995) in *Measurement and Manipulation of Intracellular Ions* (Kraicer, J., and Dixon, S. J., Eds.) pp 52−68, Academic Press, San Diego.

BI9826355